

Regimes of the Pomeron and its Intrinsic Entropy

Edward Shuryak and Ismail Zahed

*Department of Physics and Astronomy,
Stony Brook University,
Stony Brook, NY 11794, USA*

We suggest that the perturbative and non-perturbative descriptions of the Pomeron can be viewed as complementary descriptions of different phases in the Pomeron phase diagram, with a phase boundary where the proper description of the produced systems are “string balls”. Their intrinsic entropy is calculated and turned out to be the same, as the recently reported perturbative entanglement entropy. The distribution of large multiplicities stemming from the string balls is also wide, with its moments close to those reported for hadrons in pp collisions at the LHC. At low- x , the quantum string is so entangled that sufficiently weak string self-attraction can cause it to turn to a string ball dual to a black hole. We suggest that low- x saturation occurs when the density of wee-strings reaches the Bekenstein bound, with a proton size that freezes with increasing rapidity. Some of these observations maybe checked at the future eIC.

I. INTRODUCTION

Already in the 1960’s high energy hadronic collisions were described using “Reggeon exchanges” with various quantum numbers. The *Pomeron*, named after Pomeranchuk who introduced the leading exchange with vacuum quantum numbers, dominates hadronic collisions at high energies. Phenomenological descriptions of weakly interacting Pomerons have been developed by Gribov and collaborators, see [1, 2].

In the 1970’s, with the advent of QCD in its weak coupling form, a lot of work has been devoted to describe high energy collisions by re-summing certain gluonic Feynman diagrams. This program has been, to leading order, completed by Balitsky, Fadin, Kuraev and Lipatov [3] and is known as the BFKL Pomeron. Reformulation of it in terms of Wilson loops, and the addition of the nonlinear effects leading to saturation, has lead to the so called BK equation, due to Balitsky and Kovchegov [4].

While the perturbative description is valid at small distances, hadronic collisions deal with object sizes and impact parameters ~ 1 fm, where nonperturbative effects due to confinement are dominant. Therefore multiple efforts have been made to develop a “non-perturbative Pomeron”. In this work we discuss one of such approaches, developed using semiclassical tunneling and an effective long string action by Basar, Kharzeev, Yee and Zahed [5], for brevity

to be called BKYZ Pomeron. Its main elements will be presented in the next section.

(We will not review other versions of non-perturbative Pomerons, and just note in passing that a holographic idea relating the Pomeron to a dual graviton exchange [6] has evolved into a rather successful theory of double-diffractive production [7, 8] in a framework of AdS/QCD.)

In a previous paper by the two of us [10], to be referred to below as I, it was pointed out that the stringy Pomeron possesses an *intrinsic temperature and entropy*. It happens because the classical world-volume of the exchanged string, for brevity to be called a “tube”, possesses a periodic coordinate, which can be identified with a Matsubara time. Therefore quantum oscillations of the tube have the form of a thermal theory. This temperature depends on the location along the tube, its maximal value is

$$\frac{1}{T} = \beta = \frac{2\pi b}{\chi}, \quad (1)$$

where b is the impact parameter (the length of the tube) and $\chi = \ln(s/s_0)$ is the relative rapidity of the beams. In the standard way, this temperature defines the energy, entropy and other thermodynamic quantities of the system.

Further arguments in I point out that since the QCD strings are well known to exhibit the so called Hagedorn transition as a function of temperature, real or “effective”, at a certain temperature T_H . As $T \rightarrow T_H$ from below,

the string gets excited and becomes very long. Its energy E is however cancelled by the entropy term in the free energy $F = E - TS$, keeping F small. Such behavior of strings as a function of T in pure gauge theories has been studied in detail, with the conclusion that T_H is only slightly higher than the critical temperature $T_c \approx 270$ MeV (for the $SU(3)$ color group). Below we will find that the Pomeron as a twisted tube carries a lower intrinsic Hagedorn temperature.

Studies of the so called “elastic scattering profile function” $F(b)$ in I, have identified three distinct regimes: (i) a “cold string” at large b , in which $F(b) \sim \exp(-b^2)$ due to the dominant classical action of the string; (ii) a “near-critical string” at intermediate b , in which the amplitude grows as $F(b) \sim \exp(-\sqrt{1 - b^2/b_c^2})$; and an “over-excited string” at $b < b_c$ or $T > T_H$ in which the nucleon is effectively black with $F(b) \sim 1$. All three regimes are clearly seen in the LHC data on $F(b)$, see Fig. 4 of I.

While the paper I was devoted to description of the *elastic* pp collisions, we now try to extend the notion of three regimes of the Pomeron to the *inelastic* collisions. But, before we proceed with this task, we need to mention several important works which influenced our thinking.

The highly excited string state has been described in [11, 12] in terms of the so called *string balls*. This notion which originated from the string theory literature, describes a self-interacting string system that interpolates between a free string at small mass, and a black hole at large mass. We will continue along this line in section VI.C below.

Another development, triggering the present paper, is due to Kharzeev and Levin [13]. In this work, devoted to a perturbative BK-like description of the Pomeron, the authors pointed out that the produced system of gluons has certain distribution over the gluon number P_N and thus certain *intrinsic entropy* (but no temperature!). Let us for clarity explain that the term “intrinsic” here and elsewhere is used to emphasize that it is developed prior to the collision, to distinguished it from the “final entropy” related to the system of hadrons observed in the detectors. While P_N itself has been derived previously, Kharzeev and Levin successfully compared it to the distribution over *hadronic* multiplicity in pp collisions. They have also noted

that since the gluon production is modeled by a kinetic equation, one can make statements about the entropy growth as a function of the effective evolution time, or $\ln(s)$, leading eventually to a state of maximal possible entropy.

The most important feature is that the two versions of the Pomeron, BFKL and BKYZ ones, starting from very different Lagrangians and views on the underlying dynamics, end up with the very same expressions for the Pomeron elastic amplitude (modulo parameters). The aim of this paper is to discuss the similarities and differences between these two theories, extending the discussion to *inelastic* collisions. The central stage in it will be taken by the notion of the “intrinsic entropy”, the notion of “string bits” and the distributions over them.

II. THE BKYZ POMERON

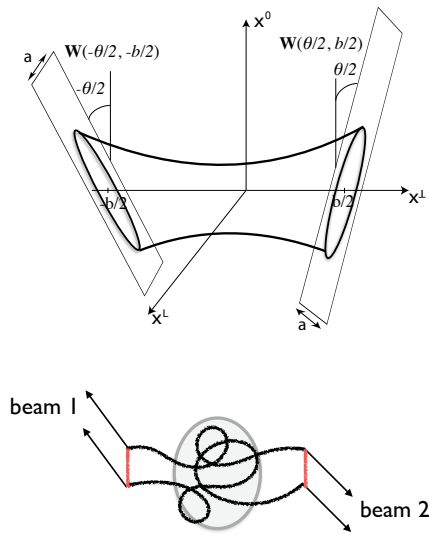


FIG. 1: The BKYZ Pomeron as a close quantum string exchange between two dipole sheets in Euclidean space (top). The same exchange when cut horizontally (bottom) from [10].

The perturbative BFKL Pomeron is based on a partonic shower, with the elementary process being a splitting of a gluon into two gluons.

The formulation of Mueller and his collaborators [17] modifies it into a splitting of one dipole into two, by production of pair of charges. The “stringy” BKYZ Pomeron describes the same basic process of a charge pair creation, but in the confining phase of QCD, in which most of their energy is in the confining strings (the QCD flux tubes).

Let us sketch the main steps of the derivation of the BKYZ Pomeron amplitude in a graphical form. The upper plot in Fig.1, from [5], is a sketch of the string world volume describing its Euclidean time history, for brevity to be called a “tube”. It is a minimal area surface (think of a twisted soap film) interpolating between the two “holes” produced in the rectangular world-volume spanned by the strings, residing in both passing dipoles. Cut vertically, it is understood as a virtual exchange of a closed string (a virtual glueball) between the dipoles. Cut horizontally (see the lower plot in Fig.1, also from [5]) it is a process creating a pair of strings.

The derivation starts with the standard approximation, in which the protons are viewed as quark-diquark dipoles, “frozen” at high energies and represented by Wilson loops running along two respective light cones. Specifically, the scattering amplitude for the process $1 + 2 \rightarrow 3 + 4$ at large \sqrt{s} factorizes [14]

$$\begin{aligned} \mathcal{T}_{12 \rightarrow 34}(s, t) &= -2is \int \frac{dz_1}{z_1} \frac{dz_2}{z_2} \\ &\times \psi_{34}(z_1) \psi_{12}(z_2) \mathcal{T}_{DD}(\chi, \mathbf{q}_\perp, z_1, z_2) \end{aligned} \quad (2)$$

where z_i is related to the transverse size of the i-dipole element described by the wave function ψ_i . The dipole-dipole scattering amplitude is given by

$$\mathcal{T}_{DD}(\chi, \mathbf{q}_\perp, z_1, z_2) = \int d\mathbf{b}_\perp e^{i\mathbf{q}_\perp \cdot \mathbf{b}_\perp} \mathbf{W}\mathbf{W} \quad (3)$$

with the Wilson loop correlator

$$\mathbf{W}\mathbf{W} \equiv \langle \mathbf{W}(C_1) \mathbf{W}(C_2) \rangle - 1 \quad (4)$$

and the normalization $\langle \mathbf{W} \rangle = 1$. The Wilson loops are evaluated along closed rectangular surfaces $C_{1,2}$ lying on the light cone, at an impact parameter b . Fig. 3 gives an illustration of the set up in Euclidean space with the

identification $\theta \rightarrow i\chi$ in Minkowski space. The averaging in (4) is over the Yang-Mills gauge fields. This correlator can be calculated either in 4-d flat space, or, using holography at strong coupling, in 5-d deformed AdS_5 .

For 2 incoming dipoles of identical size a_D the result for $b > \beta$ is [5, 15]

$$\mathbf{W}\mathbf{W} \equiv -\frac{g_s^2 a_D^2}{4\alpha'} \mathbf{K}_T(\beta, b) \quad (5)$$

where the transverse partition function

$$\begin{aligned} \mathbf{K}_T(\beta, b) &= \\ &\left(\frac{\pi}{\chi}\right)^{\frac{D_\perp}{2}} e^{-\sigma\beta b} \text{Tr} \left(e^{-2\chi \left(\mathbf{L}_0 - \frac{D_\perp}{24}\right)} \right) \end{aligned} \quad (6)$$

sums up the transverse oscillator modes in flat D_\perp , and $\sigma_T = 2\sigma$. Here g_s is the string coupling. The tracing is over the eigenmodes of the tube, over the zero point oscillations (known as the tachyon) plus the transverse excitations. The normal ordered Virasoro generator \mathbf{L}_0

$$\mathbf{L}_0 = \sum_{n=1}^{\infty} \sum_{i=1}^{D_\perp} : a_{-n}^i a_n^i : \quad (7)$$

plays the role of the Hamiltonian, with a_n^i satisfying the transverse oscillator algebra

$$[a_n^i, a_m^j] = n \delta^{ij} \delta_{n+m,0} \quad (8)$$

The normal ordering in (7) produces the zero-point contribution with the central charge of the bosonic string $C = D_\perp$, the number of transverse dimensions (2 or 3, depending on the setting). The excited modes correspond to the so called Pomeron daughters (see a brief discussion of those in Appendix B).

In pQCD the physical picture explaining why the hadronic cross sections grow with energy, is known as Gribov diffusion. In it $\chi = \ln(s/s_0)$ plays the role of time: as it grows, the gluons spread in the transverse plane diffusively $r_\perp^2 \sim \chi$. The stringy Pomeron predicts the same phenomenon, and in fact the amplitude (6) satisfies the diffusion equation

$$(\partial_\chi - \Delta - \mathbf{D}\nabla_{\mathbf{b}_\perp}^2) \mathbf{K}_T = 0 \quad (9)$$

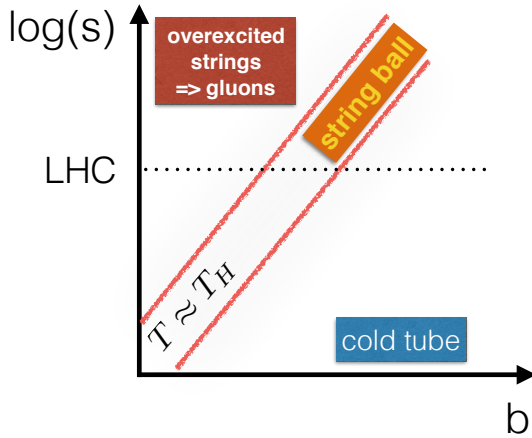


FIG. 2: The Pomeron “phase diagram”.

with the Pomeron intercept $\Delta = \alpha_P - 1$

$$\Delta = \frac{D_\perp}{12} - D_\perp \sum_{n=1}^{\infty} \frac{n}{e^{2\chi n} - 1} \rightarrow \frac{D_\perp}{12} \quad (10)$$

and a diffusion constant $\mathbf{D} = \alpha'/2$. (Note that $\alpha' = 0$ in pQCD.)

Furthermore, a holographic approach promotes this diffusion, from the two-dimensional transverse plane to a three-dimensional space $D_\perp = 3$, including the holographic coordinate z . If appropriately modified by dilaton background, it can nicely describe the transition from the weak coupling at small z , to strong coupling and confinement at large z [16]. A consequence is the following correction to the Pomeron intercept

$$\Delta \rightarrow \Delta(\lambda) = \Delta - \frac{(D_\perp - 1)^2}{8\sqrt{\lambda}} \quad (11)$$

with large 't Hooft coupling $\lambda = g^2 N_c$ in the denominator.

By approximating it by a conformal AdS space, and identifying the size of the dipoles with their locations in z , Stoffers and Zahed [9] generalized the stringy Pomeron to the treatment of deep inelastic ep scattering, in which one of the dipoles – originated from a highly virtual photon with large Q^2 – has a very small size $\sim 1/Q$. They have shown that this generalization can describe well the famous HERA data.

III. THE “PHASE DIAGRAM” OF THE BKYZ POMERON

The effective temperature of the string world-sheet is identified with the inverse β already given above (1). One physical interpretation of it can be made by noticing that the string tension causes its end-points to recede from each other with a relative acceleration $a_U = \chi/b$, thus inducing the so called Unruh temperature $a_U/2\pi$ associated with accelerated frames on the string world-sheet. Note that the effective temperature is larger for a small impact parameter b (central collisions) or large relative rapidity χ (large boosts).

The expressions above were established using the Polyakov-Luscher action for long strings with $b \gg \beta$ in flat $2 + D_\perp$ dimensions, for which the tube fluctuations are small. However, as T approaches the Hagedorn temperature here defined using $\sigma = \sigma_T/2$

$$T_H = \frac{1}{\beta_H} = \left(\frac{3\sigma}{\pi D_\perp} \right)^{\frac{1}{2}} \quad (12)$$

the fluctuations increase strongly. For $D_\perp = 3$ and $\alpha' = 1/2\pi\sigma_T \sim 1/\text{GeV}^2$, the intrinsic Hagedorn temperature is $T_H \sim 160$ MeV for the Pomeron, which is lower than the Yang-Mills Hagedorn temperature ~ 270 MeV as we noted earlier. It is remarkably close to the reported QCD chiral cross-over transition temperature. In this regime, using the Nambu-Goto action instead, we have derived the resummed action [10],

$$\mathbf{K}_T(\beta, b) \rightarrow \left(\frac{\pi}{\chi} \right)^{\frac{D_\perp}{2}} \text{Tr} \left(e^{-\sigma\beta b \left(1 + \frac{24}{D_\perp} \frac{\beta_H^2}{\beta^2} \left(\mathbf{L}_0 - \frac{D_\perp}{24} \right) \right)^{\frac{1}{2}}} \right) \quad (13)$$

Its dual relation to the static potential, especially its Arvis form, is discussed in Appendix A. Note that (13) returns to (6) in the “cold” regime with $\beta \gg \beta_H$ and $2b > \beta_H$.

For deep inelastic scattering (DIS) one often uses the kinematic range plot of the $\ln(Q^2) - \ln(\frac{1}{x})$ variables, where the regions of weakly

coupled vs strongly coupled domains, and saturated vs dilute parton ensembles are identified. Let us summarize this section with a similar diagram for the ‘‘Pomeron phase diagram’’. It is in quotation marks because the system in question – two colliding hadrons or dipoles – is not really macroscopic, so there is no true phase transition related to thermodynamical singularities in this phase diagram.

Our plot, shown in Fig. 2, is in the $b-\ln(s/s_0)$ plane. The transition region in the middle corresponds to the near-critical regime defined by the equation $T \approx T_H$ where T was given in (1) and the intrinsic Hagedorn temperature for the Pomeron in (12). While at LHC energies, indicated by a horizontal dotted line, all three regions are clearly visible, at lower ones (RHIC/ISR colliders) only the ‘‘cold’’ regime is present and the elastic collisions profile is basically Gaussian. For orientation, at LHC the gray transition region is for b between 0.5 and 1 fm. This is to be compared with the ‘‘typical impact parameter $\sqrt{\sigma_{tot}/\pi} \approx 1.5$ fm. Note further, that while all three regions have comparable size in terms of b , their contribution to the cross section scales as b^2 weighted with the profile, and therefore the central black region still provides a rather small contribution to it.

IV. THE INTRINSIC ENTROPY OF THE POMERON

In QED a moving charge or dipole carries ‘‘Weizsaecker-Williams’’ field with it. In perturbative QCD it is substituted by a cloud of gluons, produced by subsequent gluon splittings. As pointed out by Kharzeev and Levin [13], the perturbative gluon cascade leads to some rather interesting results, which we briefly summarize now.

First, they found that the (von Neumann) entropy is just linear in $\chi = \ln(s/s_0)$, with the coefficient being the Pomeron intercept

$$\mathcal{S}(x) = \Delta \chi \equiv \Delta \ln \left(\frac{1}{x} \right) \quad (14)$$

Second, the partonic cascade leads to a very wide distribution over the gluon number n , with a tail toward large multiplicities

$$\begin{aligned} P_n(\chi) &= e^{-\Delta\chi} (1 - e^{-\Delta\chi})^{n-1} \\ &= \frac{1}{\bar{n}} \left(1 - \frac{1}{\bar{n}} \right)^{n-1} \end{aligned} \quad (15)$$

of the form known in statistics as a negative binomial distribution.

The third important point made by Kharzeev and Levin is that this distribution in fact describes the distribution over *hadron multiplicity* observed in pp collisions at LHC. This statement is demonstrated by calculating the moments of the distribution

$$C_q = \frac{\langle n^q \rangle}{\langle n \rangle^q} \quad (16)$$

Their experimental values

$$C_2^{exp} = 2.0 \pm 0.05, \quad C_3^{exp} = 5.9 \pm 0.6,$$

$$C_4^{exp} = 21 \pm 2, \quad C_5^{exp} = 90 \pm 19$$

are close to their theoretical predictions $C_2 \approx 1.83, C_3 \approx 5.0, C_4 \approx 18.2, C_5 \approx 83$. This observation is proposed as an evidence for the final hadrons being produced from the gluon cascade.

Let us now proceed to the issue of the intrinsic entropy of the stringy tube. We will give first the most direct (thermal) derivation of it. The thermal free energy associated with the stringy tube is $\mathbf{F} = -T \ln \mathbf{K}_T$, for the temperature $T = 1/\beta$. The corresponding thermal entropy is, by definition,

$$\mathcal{S}_P = \beta^2 \frac{\partial}{\partial \beta} \left(-\frac{\ln \mathbf{K}_T}{\beta} \right) \quad (17)$$

In flat space, we can differentiate (6) and obtain

$$\begin{aligned} \mathcal{S}_P &= D_\perp \sum_{n=1}^{\infty} \ln \left(1 + \frac{1}{e^{2\chi n} - 1} \right) \\ &+ 2\chi \left(\frac{D_\perp}{12} - \sum_{n=1}^{\infty} \frac{n}{e^{2\chi n} - 1} \right) \\ &- \frac{D_\perp}{2} \left(1 + \ln \left(\frac{2\chi}{2\pi} \right) \right) \end{aligned} \quad (18)$$

At large collision energy $\chi \rightarrow \infty$ the leading contribution is the linear term in the second line

$$\mathcal{S}_P \approx 2\chi \frac{D_\perp}{12} \rightarrow 2\chi \Delta(\lambda) \equiv 2 \ln \mathbf{N} \quad (19)$$

(with the rightmost relation following from the diffusion in curved space as will be detailed shortly).

The derived entropy corresponds to the elastic amplitude, with a “tube” or two exchanged strings. The optical theorem tells us that it corresponds to the cross section, or the inelastic amplitude *squared*. This means that the inelastic amplitude has *one* string, or half a Pomeron, and thus half of the entropy. We thus conclude that the intrinsic entropy of the inelastic pp collision is

$$\mathcal{S}_{\text{inelastic}} = \chi \Delta(\lambda) \quad (20)$$

Note, that this main result, the intrinsic entropy of the stringy Pomeron, turns out to be *the same* as that of the gluon cloud (14), provided that the Pomeron intercept Δ is changed appropriately.

V. DISTRIBUTION OF STRING BITS

In the original stringy Pomeron approach only the elastic amplitude has been calculated, via a semiclassical “tube” in Euclidean time describing the tunneling event. At this level, the intrinsic temperature and entropy we discussed above are just technical parameters describing quantum oscillations of the tube. Elastic scattering still deals with one quantum state, and thus zero entropy.

In order to proceed to inelastic collisions, one needs to develop certain analog of the “Cutkosky’s cutting rules”, allowing to implement unitarity and representing the imaginary part of the elastic amplitude as a total cross section, the sum over the probabilities to produce all physical final states. We have already shown it schematically, as a transition from the upper to the lower sketch in Fig.1.

After the intrinsic entropy is derived, let us now propose a distribution over the number and locations of the “string bits” (or “wee-strings”) produced by the BKYZ Pomeron.

We propose to quantify this in the following way. Keeping in mind the holographic extension of the stringy Pomeron already mentioned, one needs to “amputate” the string ends, associated with the colliding dipoles. Technically it

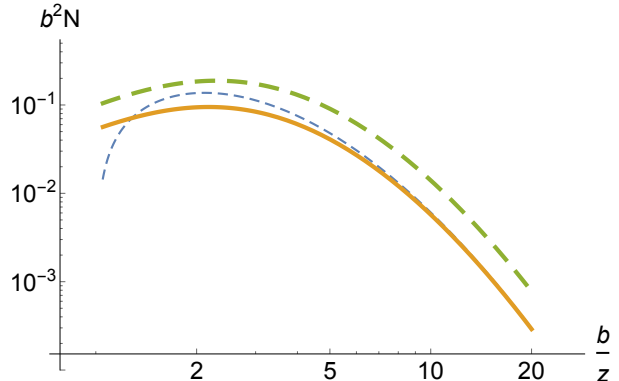


FIG. 3: Density distribution of string bits of fixed size $z = 0.9 z_0$ at a transverse distance b/z , as sourced by a dipole of size $z' = 0.9 z_0$ at the origin at a relative rapidity $\chi = 10$. The middle-blue-dashed curve is (23) and follows from the large b -asymptotic of the lower-orange-solid curve for AdS without a wall (first contribution in (C3)). The upper-green-long-dashed curve is the full (C3) for AdS with a wall.

leads to the (dimensionless) *density of string-bits* identified with

$$\mathbf{N} \approx \frac{z_0^2 \mathbf{K}_T}{z z'} \quad (21)$$

with $0 \leq z \leq z_0$ identified as the holographic direction, as we recall in Appendix C. It satisfies a diffusion equation as well, and therefore also satisfies the “chain rule”

$$\mathbf{N}(3, 1) = \int d^2 \mathbf{N}(3, 2) \mathbf{N}(2, 1) \quad (22)$$

It is a necessary feature of a cascade, which can always be split into two subsequent cascades if some “measurement” needs to be done, at some intermediate time.

This density describes a cloud of string bits, in analogy to the cloud of gluons. However, there is a significant difference: the string bits are not independent, in fact they together form continuous QCD strings, stretched between the probe and the target dipoles, as shown in the lower plot of Fig. 1 and also in Fig. 4a.

In the perturbative BFKL ladder diagrams, on the other hand, the produced gluons are ordered only in their longitudinal rapidities. While their transverse locations are also defined

relative to those of the neighboring “rungs” of the ladder, the corresponding integrals have a logarithmic measure $\sim dx_{\perp}^2/x_{\perp}^2$ allowing large jumps, illustrated in Fig. 4b. Instead of a continuous string, pQCD predicts essentially randomly placed gluons, with color indices uncorrelated with positions. This create practical problems and ambiguities in event generators, such as the Lund model and its descendants.

The density of string bits can be found in closed form for AdS without and with a wall as we detail in appendix C. For small dipoles sizes or $\mathbf{b}_{\perp}^2/2zz' \gg 1$, it takes the simple form

$$\mathbf{N}(\chi, z, z', b) \approx 2 \frac{e^{\Delta(\lambda)\chi}}{(4\pi\bar{\mathbf{D}}\chi)^{3/2}} \times \frac{zz_0^2}{z'b^2} \ln\left(\frac{b^2}{zz'}\right) e^{-\ln^2\left(\frac{b^2}{zz'}\right)/(4\bar{\mathbf{D}}\chi)} \quad (23)$$

with

$$\bar{\mathbf{D}} = \frac{\mathbf{D}}{z_0^2} \rightarrow \frac{1}{2\sqrt{\lambda}} \quad (24)$$

\mathbf{N} is the density of *string bits* of size z at a transverse distance $b = |\mathbf{b}_{\perp}|$ sourced by a dipole of size z' located at the origin. In Fig. 3 we show the density distribution of string bits (23) as the middle-blue-dashed curve as a function of the distance b/z in the transverse plane, for $\chi = 10$, $z = z' = 0.9z_0$ and $\lambda = 23$. The lower-orange-full curve is the unexpanded distribution without the AdS wall or the first contribution in (C3), and the upper-green-long-dashed curve is the full distribution in walled AdS as given in (C3). The total number of string bits is

$$\mathbf{N} = \int \frac{dz}{z} \frac{d\mathbf{b}_{\perp}}{z_0^3} \frac{z'\mathbf{N}}{z_0} = e^{\Delta(\lambda)\chi} \quad (25)$$

The total number of string bits thus grows exponentially with χ , or as a power Δ of the collision energy. Note that the number and distribution of string bits (23) is conspicuously similar to the distribution of small dipoles in the perturbative BFKL equations [17] (again, modulo the substitution of the Pomeron intercept).

While it is not really necessary, let us at the end of this section present another – perhaps more intuitive – way to visualize this virtual

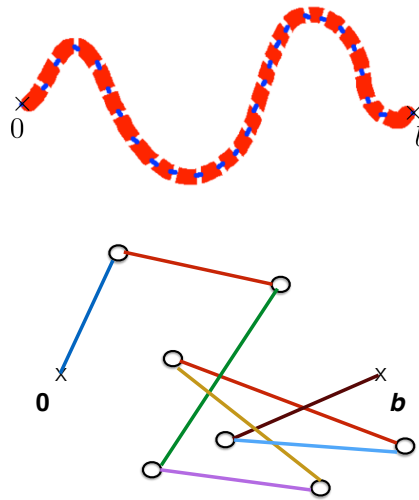


FIG. 4: (a) String bits in a stringy Pomeron, exchanged at fixed impact parameter b . (b) Gluons are indicated by small circles in the transverse plane, as emitted from a BFKL ladder diagram. In the limit of a large number of colors $N_c \rightarrow \infty$, the colors are unique for each gluon, and there is one unique way to connect them by color fluxes. Since in pQCD there is little correlation between the gluon positions, the overall string length needed is much longer.

cloud of string bits in transverse space. For a string with fixed end-points the transverse string coordinate $x_{\perp}^i(\sigma, \tau)$ can be discretized into $N + 1$ points located at $0 \leq \sigma = k\pi/N \leq \pi$ with $k = 0, \dots, N$ for each $i = 1, \dots, D_{\perp}$,

$$x_{\perp}^i\left(\frac{k\pi}{N}, \tau\right) = \frac{\mathbf{b}^i}{\pi} \frac{k\pi}{N} + \sum_{n=1}^{N-1} X_n^i(\tau) \sin\left(n \frac{k\pi}{N}\right) \quad (26)$$

The string amounts to a collection of N string bits, or beads in the transverse space as illustrated in Fig. 4. A similar interpretation for open strings on the light-cone was suggested in [19]. Normalization of the number of string bits is the same as counting the number of stationary waves. (Note that this counting is reminiscent of Debye counting of phonons in solids.)

For large b , the Hamiltonian for the amplitudes X_n^i of the stationary modes, follows from the Polyakov-Luscher action as a collection of

$N - 1$ free oscillators in D_\perp dimensions

$$\frac{1}{2} \sum_{n=1}^{N-1} \left(\dot{X}_n^i(\tau) \dot{X}_n^i(\tau) + n^2 X_n^i(\tau) X_n^i(\tau) \right) + \frac{b^2}{\pi^2} \quad (27)$$

The ground-state wave-function for this dangling string is made of zero point contributions

$$\Psi_N[X] = \prod_{i=1}^{D_\perp} \prod_{n=1}^{N-1} \left(\frac{n^2}{\pi} \right)^{\frac{1}{4}} \exp \left[-\frac{n^2}{2} (X_n^i)^2 \right] \quad (28)$$

where all configurations with any number of string modes n are equally probable. Therefore the probability per configuration is $p_n = 1/(N - 1)$. The zero-point fluctuations on the string are maximally entangled, with an intrinsic von Neuman entropy

$$\mathcal{S} = - \sum_{n=1}^{N-1} p_n \ln p_n = \ln N_{wee} \quad (29)$$

Finally, let us briefly consider the process of *hadronization*. In a perturbative approach this leads to a well known difficulty: gluons have color indices, and eventually need to confront color confinement at large distances. Event generators as used in practice, such as the Lund model and its descendants, use certain stochastic algorithms for connecting gluon color indices by strings. The number of possible connections is very large and these algorithms are rather arbitrary. Furthermore, their modifications – known as “color reconnections” – do affect the results.

In the stringy Pomeron model one can quantify such rules. We propose to use for the produced strings the density of “wee-strings” (21), or its confined form in walled AdS in (C3).

A. Large multiplicity events

As we already mentioned earlier, in practice in pp collisions it is so far impossible to determine the value of the impact parameter b for inelastic events. Therefore, one needs to integrate over b , and, since our phase diagram suggests three different regimes for different b ,

the question is which one of the three, “black”, “gray” or “dilute”, is the dominant one, for the high multiplicity tail.

According to Kharzeev and Levin [13], it is the perturbative small- b domain. According to Bjorken, Brodsky and Goldhaber [21], it is the large- b or cold string domain. (This is motivated by the fact that in this case the elliptic deformation parameter is as large as it can be, $\epsilon_2 \sim 1$, thus maximizing the elliptic flow.)

In contrast, we propose that the tail of the multiplicity distribution may be dominated by the “gray” or near-critical regime in our Pomeron phase diagram (Fig. 2). In this case the amplitude, in this so called Hagedorn regime, is

$$\mathbf{K}_T(\beta, b) \sim e^{-\beta \mathbf{F}_0} \sim e^{-\sigma \beta b} \left(1 - \frac{\beta_H^2}{\beta^2} \right)^{\frac{1}{2}} \quad (30)$$

with a vanishingly small free energy \mathbf{F}_0 in the amplitude. However, there are both a large energy (string mass) $M = -\partial \beta \mathbf{F}_0 / \partial \beta$, and a large entropy, which conspire to cancel out. The string length is large $L / \sqrt{\alpha'} = \beta^2 \partial \mathbf{F}_0 / \partial \beta$

$$L \sim M \alpha' \sim \frac{b \sqrt{2}}{4\pi} \left(1 - \frac{\beta_H}{\beta} \right)^{-\frac{1}{2}} \quad (31)$$

and the partition function takes the Hagedorn form

$$\mathbf{K}_T(\beta, b) \sim e^{\beta_H L / \alpha'} e^{-\beta M} \quad (32)$$

in which long strings are distributed *thermally* as $e^{-\beta M}$. We speculate that events with initially long strings also carry large hadron multiplicities at the end of the collisions $N_L = M \sqrt{\alpha'} \gg 1$ when they hadronize. In the inelastic collision the string bits come out of the critical Pomeron, like beads coming out of a shattered neckless. Each string bit is a colorless closed string or glueball of typical mass $1/\sqrt{\alpha'} \sim 1$ GeV, which can break into several pions, for $T = 1/\beta$ close to $T_H \sim 160$ MeV as defined in (12). The normalized distribution for the events with large multiplicity N_L is therefore thermal

$$P(N_L) = \frac{1}{N_L} e^{-N_L / \bar{N}_L} \quad (33)$$

after fixing β to reproduce the mean charged particle multiplicity which by our stringy estimates is

$$\bar{N}_L = \frac{2}{3} \times 7 \times \mathbf{N}_{\text{wee}} = \frac{14}{3} \left(\frac{s}{s_0} \right)^{\Delta(\lambda)} \quad (34)$$

The fluctuations of the multiplicity distribution following from (33) are given by the thermal cumulants

$$C_q = \frac{\langle N_L^q \rangle}{\langle N_L \rangle^q} = q! \quad (35)$$

If so, one finds values for the first four moments, $C_q = 2, 6, 24, 120, \dots$ also close to the experimental ones given at the beginning of the section, inside the errors. We interpret this agreement as an argument, that the final hadrons *may* come from the near-critical string-balls. Admittedly, at the time of this writing there is no proposal how to separate our and Kharzeev-Levin scenarios experimentally.

VI. SUMMARY AND DISCUSSION

A. Summary

Before we summarize the paper, let us once again remind the reader of what was known before it.

The most nontrivial fact is that the scattering amplitude has the same Pomeron form, both in the weak coupling BFKL theory, and in the stringy BKYZ one. Gribov diffusion of gluons turns out to be quite similar to a diffusive propagation of a virtual string. Both makes the hadron sizes grow at high energies. This has been shown in [5].

The next important point, from [10], is about the difference between the two. The stringy tube has a periodic coordinate, and thus an effective temperature and entropy. Furthermore, one can identify the existence of the new intermediate regime, related to Hagedorn-like string excitation. It has been identified in the elastic profile $F(b)$.

Kharzeev and Levin [13] described gluon production by a kinetic equation, and pointed out

that the gluons produced have a very wide distribution in multiplicity, very similar to the distribution over hadrons. As the distribution is calculated, one can also calculate the “intrinsic entropy” of the system.

Our main point now is that since in inelastic collisions there is (so far) no means to define the impact parameter b , one has to integrate over it. As a result, *all three* regimes of the BKYZ Pomeron, as a function of b , seen in elastic collisions, should also contribute to its intrinsic entropy. The distribution in the number of gluons in pQCD domain needs to be complemented by a study of the distribution over the lengths and shapes of the promptly produced “string balls” at intermediate b and the “cold strings” at large b .

We find the intrinsic entropy of the string to be very similar to that found perturbatively. We found that the distribution over string-bits multiplicity is also very wide, and its moments are also close to the experimental ones. So, whether the observed high-multiplicity events originate from the gluonic cascade or long near-critical string balls, remains to be studied further.

B. How smooth is the transition between the weak and strong coupling regimes?

While above we have emphasized the similarities between the BFKL and BKYZ Pomerons above, now is the time to discuss their differences. While the entropy may be similar, only the second one has an effective temperature. Furthermore, only the second one hints at the existence of the intermediate near-critical regime, and on the fact that two sides of our “phase diagram” are separated by something resembling a first order transition, like in thermal gluodynamics.

The question at the title of this subsection can be specified further: Do all the Pomeron parameters join smoothly, or can there be some observable remnants of the Hagedorn phase transition?

In pQCD the Pomeron intercept in the leading order is

$$\Delta_{BFKL} = \frac{4}{\pi} \alpha_s N_c \ln 2 \quad (36)$$

The next order $\alpha_s^2 N_c^2$ correction [22] gets substantial at $\alpha_s \approx 0.08$ or 't Hooft coupling $\lambda = g^2 N_c \approx 3$.

In the stringy BKYZ version in the holographic setting and large λ , the intercept is (11)

$$\Delta_{BKYZ} = \frac{D_\perp}{12} - \frac{(D_\perp - 1)^2}{8\lambda} \quad (37)$$

where the number of transverse dimensions is holographically $D_\perp = 3$. The second contribution contains the large coupling $\lambda = 4\pi\alpha_s N_c$, is a correction induced by the curvature of AdS. Note that (like all one-loop semiclassical effects) the first leading term is independent of the coupling and is just a number $\Delta = \frac{1}{4}$, being close to the empirical power observed in pp and DIS. Note further, that this limit is reached at very strong coupling *from below*. So, this trend agrees at least in sign with the weak coupling BFKL result, and in principle those two can join smoothly. A rough estimate of the cross-over coupling α_{s*} for which this is expected to take place can be inferred from the leading order contributions if there is no jump in the intercept,

$$\alpha_{s*} \sim \frac{\pi D_\perp}{48 N_c \ln 2} \sim 0.1 \quad (38)$$

C. The size and shape of the Pomeron and the interacting string balls

A very massive string can only behave as a black hole if its self-attraction is taken into account [23, 24]. The objects, interpolating between free strings at small masses and black holes at large ones, are known as *string balls*. Their generic properties in the string theory context have been given by Damour and Veneziano [24].

Its application to high multiplicity hadron collisions has been proposed in [10]. Detail studies of QCD string balls started in [11]. In it the evidences for self-interaction of QCD strings from lattice studied have been reviewed, with the conclusion that it is, like gravity, attractive, and is generated by an exchange of (scalar isoscalar) σ -meson exchange. Unlike gravity, it has a finite range $1/m_\sigma \approx 1/600 \text{ MeV} \sim 0.3 \text{ fm}$. The same conclusion has been reached in [25],

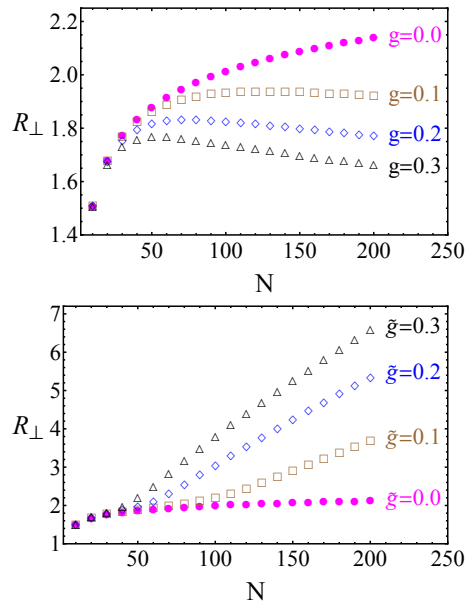


FIG. 5: String transverse sizes for attracting self-interactions (top) and repulsive self-interactions (bottom) from [12].

in which the holographic AdS/QCD model has been used to describe the QCD strings and their interactions. See also a holographic model discussed in [20].

Numerical simulations of the QCD string-ball properties have been performed in [11, 12], via certain discretized models. One can reproduce strong free string excitations near the Hagedorn temperature $T \rightarrow T_H$, and then probe how self-interactions affect the string system. Another issue studied there has been shape fluctuations of the string balls, described by azimuthal angular moments $\epsilon_m = \langle \cos(m\phi) \rangle$, which (for large enough multiplicity) can be converted by collective flows to observed angular moments of particle distributions v_m .

Here we would only describe, in Fig. 5, how the transverse sizes of a self-interacting stringy Pomeron depend on the interaction strength, from the exploratory study in [12]. It is based on the discretized form (26-28). When the string self-attracts, the (squared) transverse size changes from being proportional to the effective time ($\chi \sim \log(s/s_0)$) growth, typical of diffusion, to a fixed size. It eventually shrinks into a collapsing regime, if the attraction is too strong. One can therefore speculate, that at

some superhigh energy, Gribov diffusion and the expansion of the Pomeron size may stop.

Although we do not think this is the case, let us also explore the opposite case of a repulsive string-string interaction. The size of the self-repelling string was found in [12] to grow linearly with N . If so, the growth of the Pomeron size will continue even more rapidly than via Gribov diffusion.

While there are observed showers from cosmic ray interactions in the atmosphere at \sqrt{s} exceeding LHC by few orders of magnitude, low statistics and uncertainty about the composition of these cosmic rays does not so far allow us to quantify the corresponding pp cross section.

The final subject we would like to discuss is the intrinsic entropy and distribution of the string bits. In the critical regime of self-attracting strings, when the size levels off with increasing N , the transverse string density is

$$n_{\perp} = \frac{N}{R^{D_{\perp}}} \rightarrow \frac{1}{g_s^2} \sim \frac{1}{l_P^{D_{\perp}}} \quad (39)$$

where the rightmost result follows at the critical value of $g_s^2 N \sim 1$ with $R_{\perp} \sim N^0$. If we recall that in holography the Planck length follows from $l_P^{D_{\perp}} \sim g_s^2 \sim G_N$ in $1 + D_{\perp}$ spatial dimensions, (39) corresponds to one wee-string per Planck volume. A critical self-attracting string saturates the Bekenstein bound for the entropy $\mathcal{S}_B \sim N$ per unit area $A_{\perp} \sim R^{D_{\perp}}$, with one bit per Planck volume. The maximally entangled self-attracting string is a black hole [23]. At saturation, $g_s^2 \sim l_P^{D_{\perp}} \sim 1/N$ and the density of wee strings reads

$$n_{\perp} \sim N \sim \mathbf{N}_{\text{wee}} = \left(\frac{1}{x}\right)^{\Delta(\lambda)} \quad (40)$$

At saturation, the proton size no longer grows with rapidity $\chi = \ln(\frac{1}{x})$. It is a black disc with fixed edges. We note that in the opposite case of a self-repelling string, the transverse size increases linearly with N in strong violation of the Froissart bound.

For what critical x_{\star} one may expect to reach the black-hole limit with the cross section leveling off? While this value depends critically on the choice of g_s and the details of the string self-interaction, for the weakest coupling $g_s \sim 0.1$,

the exploratory studies shown in Fig. 5 (flat space), suggest a transition for $N_{\star} \sim 100$. Using (40) this translates to x_{\star}

$$x_{\star} \sim \left(\frac{1}{N_{\star}}\right)^{\frac{1}{\Delta}} \sim 10^{-8} \quad (41)$$

The relative rapidities currently reached at the LHC with pp collisions at $\sqrt{s} \sim 7$ TeV and for $\sqrt{s_0} \sim 1$ GeV, correspond to a relative rapidity of $\chi = \ln(s/s_0) \sim 18$. This translates to a cloud of string bits at a resolution of $x \sim 10^{-8}$.

Acknowledgements. We thank Dima Kharzeev for discussions. This work was supported by the U.S. Department of Energy under Contract No. DE-FG-88ER40388.

Appendix A: Static potential and duality of string quantization

The potential energy of a static quark-antiquark pair, separated by a distance r has been studied since the birth of QCD, via lattice simulations and quarkonia phenomenology. It is well known that at small distances it has the perturbative Coulomb-like behaviour, with the running coupling $\alpha_s(r)$, while at large distances it exhibits a linear confining potential $V_{\text{conf}} = \sigma_T r$ due to a confining string. One question to be discussed here is where and how those two regimes meet. Another, more technical one, is whether the known expressions for the static potential can be related to our expressions for the dipole-dipole scattering amplitude.

Specifically, one can address these questions by studying corrections to the leading term for the potential, both from small and large distances. We will follow the latter and recall that the quantum vibrations of the QCD string leads to the so called ‘‘Luscher term’’ [18]

$$V_{\text{Luscher}}(r) = \sigma_T r - \frac{\pi}{12} \frac{1}{r} + \dots \quad (A1)$$

with a new Coulomb-like correction, to be valid at large r . Re-summation of the quantum corrections of the Nambu-Goto string leads to the

so called Arvis potential [26]

$$V_{\text{Arvis}}(r) = \sigma_T r \left(1 - \frac{\pi}{6} \frac{1}{\sigma_T r^2}\right)^{\frac{1}{2}} \quad (\text{A2})$$

This form suggests a singularity at a distance at which the bracket vanishes. Clearly, the string description is invalid beyond this point, as it cannot produce a negative energy. The static potential of course does change sign, becoming negative at $r < 0.2$ fm.

Its behavior in the intermediate region has been studied on the lattice, at zero and non-zero temperatures, see e.g. [27]. One can use Fig. 6 of this work to answer the following two questions: (i) at which distances the effective $\alpha_s(r)$ gets smaller than the Luscher value $(3/4)(\pi/12) \approx 0.2$?; and (ii) at $T > T_c$, when the confining string is absent, at which distances one finds the same $\alpha_s(r)$? The answer to both is the same, namely $r < 0.15$ fm. One can use it as a definition of the applicability region of pQCD, for this problem.

Before turning to more technical issues, let us note that the static potential is not directly observable: spectra for quarkonia were fitted with a Cornell potential, in which $\alpha_s \sim 0.5$. Distances $r \sim 0.15$ fm do not play a particularly important role in the spectroscopy. The scattering amplitude profile $F(b)$, on the contrary, is directly observable, and it basically contains the potential energy in the exponent. That is why one can detect in it a pQCD-string transition much better than in the static potential.

Now we turn to the relationship between the expressions for the Pomeron and the static potential. In Fig. 6a we sketch the world-volume of the exchanged string in the Pomeron. Its spatial extent is the impact parameter b , and its Euclidean time extent is β (1). The semiclassical derivation assumes “cold string”, with $b > \beta$. In Fig. 6b we sketch the open string between a heavy quark-anti-quark pair propagating along the long and periodic β -direction. In this case it is assumed that the temperature goes to zero, or $b \gg \beta$.

The interplay between the Pomeron and the potential expression reflects the general conformal nature of the string action under the exchange of Euclidean time and space coordinates $\tau \leftrightarrow \sigma$. In doing so, however, one needs to pay attention to different boundary conditions

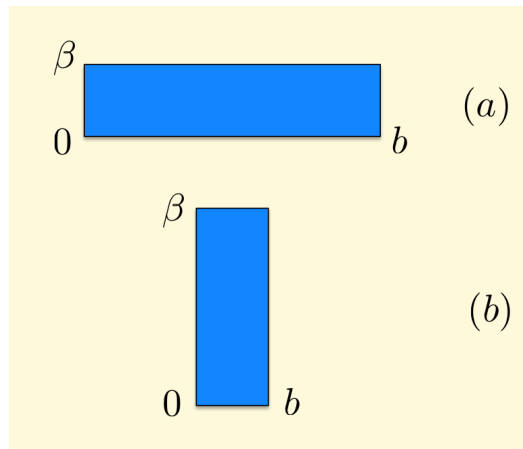


FIG. 6: The world-sheet of a Pomeron as a close string moving along the long b -direction (a), and a static quark-antiquark pair linked by an open string moving along the long β -direction (b). The world-sheets shown as rubber strips are periodic in β .

along time and space. The string is always expected to be *periodic* in time, but in space it has rigid boundary conditions, as the string is attached to locations of the Wilson lines.

The Nambu-Goto evaluation [26], corresponding to Fig. 6b, yields a partition function

$$\mathbf{Z}_T(\beta, b) = \text{Tr} \left(e^{-\sigma\beta b \left(1 + \frac{24}{D_\perp} \frac{\beta_H^2}{4b^2} \left(L_0 - \frac{D_\perp}{24}\right)\right)^{\frac{1}{2}}} \right) \quad (\text{A3})$$

It is readily seen that (A3) follows from (13) and vice se versa, under the exchange

$$2b \leftrightarrow \beta$$

The meaning of the factor 2 here is precisely due to the fact that the rigid boundary condition corresponds to “half-circle”, and only becomes a full circle (or rather a tube) if complemented by another “half-circle”. In more precise words, in order to have exact space-time duality of the two problems, one needs to double the spatial extent to have a topology of the double-torus.

Both string descriptions require the strings not to be highly excited, or $\beta > \beta_H$ as illustrated in the Pomeron phase diagram in Fig. 2.

(A3) holds for Fig. 6b for $\beta > b$ or $\chi < 2\pi$ (small rapidity), while (13) holds for Fig. 6a for $\beta < b$ or $\chi > 2\pi$ (large rapidity).

Appendix B: The regime dominated by “Pomeron daughters”

In the phase diagram, for simplicity, we have only shown one region, dominated by the near-critical string balls. However, in the lower left corner of it there exists a separate regime dominated by a different type of excitations, related to the so called “Pomeron daughters”. The amplitude (13) includes a sum not only over the zero point oscillations of the string, but also over its thermal excitations, of the type

$$\mathbf{K}_T(\beta, b) \sim \sum_n d(n) e^{-\sigma\beta b \left(1 - \frac{\beta_H^2}{\beta^2} + \frac{8\pi n}{\sigma\beta^2}\right)^{\frac{1}{2}}} \quad (\text{B1})$$

where $d(n)$ is the density of excited states. In so far we assumed $n = 0$ and ignored the Pomeron daughters with $n = 1, 2, \dots$. Now, consider what happens if $\beta < \beta_H$ when the Pomeron daughters dominate. In this case too, the strings carry large masses $M_n \sim \sqrt{n/\alpha'}$ so that (B1) becomes

$$\mathbf{K}_T \sim \sum_n d(n) e^{-2b\sqrt{2\pi\sigma n}} \sim \sum_n e^{(\beta_H - 2b)M_n} \quad (\text{B2})$$

where we used that $d(n) \sim e^{\beta_H M_n}$. So, as the distance $2b$ approaches β_H there is a separate Hagedorn transition, now induced by the multiple excitations of the Pomeron daughters.

This effect is, however, only important for low collision energies and small impact parameter $b < \beta_H/2$. Otherwise, as we discussed in the main text, the tachyon-induced second term in (B1) is dominant. In all cases, the long string distributions are thermal with an intrinsic temperature of either $1/\beta$ or $1/2b$, but the same Hagedorn temperature (12).

Appendix C: Diffusion in modified AdS_5

In the AdS/QCD models the holographic string exchange takes place in AdS_5 space,

modified by a certain profile of the dilaton field. The simplest version describing confinement, makes use of a “confining wall”, by cutting off space beyond a certain value of the holographic coordinate. The quantum version of (9) in a hyperbolic slice of AdS_{D_\perp} with line element

$$ds_\perp^2 = \frac{z_0^2}{z^2} (d\mathbf{b}_\perp^2 + dz^2), \quad (\text{C1})$$

confined to $0 \leq z \leq z_0$, follows in the form [9]

$$\left(\partial_\chi - \Delta - \frac{\mathbf{D}}{\sqrt{g_\perp}} \partial_\mu g_\perp^{\mu\nu} \sqrt{g_\perp} \partial_\nu \right) \mathbf{K}_T(x_\perp, x'_\perp) = 0, \quad (\text{C2})$$

with the short notation $x_\perp = (z, \mathbf{b}_\perp; \chi)$. Using the conformal variable $u = -\ln(z/z_0)$, the initial condition of one wee string at $\mathbf{b}_\perp = \mathbf{b}'_\perp = 0$, and the zero current condition $\partial_z \mathbf{N} = 0$ at the wall boundary $z = z_0$ (no leak at the wall), the solution to (C2) for the dimensionless density of wee strings $\mathbf{N} \approx \mathbf{K}_T / zz' / z_0^2$ is

$$\mathbf{N}(\chi, u, u', b) = e^{u'+u} \mathbb{K}_T(\chi, \xi) + e^{u'-u} \mathbb{K}_T(\chi, \xi_*) \quad (\text{C3})$$

with

$$\mathbb{K}_T(\chi, \xi) = \frac{e^{\Delta(\lambda)\chi}}{(4\pi\overline{\mathbf{D}}\chi)^{3/2}} \frac{\xi e^{-\frac{\xi^2}{4\overline{\mathbf{D}}\chi}}}{\sinh(\xi)}, \quad (\text{C4})$$

The chordal distances are

$$\begin{aligned} \cosh\xi &= \cosh(u' - u) + \frac{\mathbf{b}_\perp^2}{2z_0^2} e^{u'+u} \quad (\text{C5}) \\ \cosh\xi_* &= \cosh(u' + u) + \frac{\mathbf{b}_\perp^2}{2z_0^2} e^{u'-u}, \end{aligned}$$

with $-u$ the image of u with respect to the holographic wall at $u = 0$ ($z = z_0$). The Pomeron intercept is now (11). The density of wee-strings for AdS without a wall corresponds to only the first contribution in (C3).

-
- [1] V. N. Gribov, hep-ph/0006158; V. N. Gribov, 'Gauge Theories and Quark Confinement', 2002, PHASIS.
- [2] A. Donnachie and P. V. Landshoff, Phys. Lett. B **296**, 227 (1992) [hep-ph/9209205].
- [3] E. A. Kuraev, L. N. Lipatov and V. S. Fadin, Sov. Phys. JETP **45**, 199 (1977) [Zh. Eksp. Teor. Fiz. **72**, 377 (1977)]; I. I. Balitsky and L. N. Lipatov, Sov. J. Nucl. Phys. **28**, 822 (1978) [Yad. Fiz. **28**, 1597 (1978)].
- [4] I. Balitsky, Nucl. Phys. B **463**, 99 (1996) [hep-ph/9509348]; Y. V. Kovchegov, Phys. Rev. D **60**, 034008 (1999) [hep-ph/9901281].
- [5] G. Basar, D. E. Kharzeev, H. U. Yee and I. Zahed, Phys. Rev. D **85**, 105005 (2012) [arXiv:1202.0831 [hep-th]].
- [6] R. C. Brower, J. Polchinski, M. J. Strassler and C. -ITan, JHEP **0712**, 005 (2007) [hep-th/0603115]. R. C. Brower, M. J. Strassler and C. -ITan, JHEP **0903**, 092 (2009) [arXiv:0710.4378 [hep-th]].
- [7] S. K. Domokos, J. A. Harvey and N. Mann, Phys. Rev. D **80**, 126015 (2009) [arXiv:0907.1084 [hep-ph]].
- [8] I. Iatrakis, A. Ramamurti and E. Shuryak, Phys. Rev. D **94**, no. 4, 045005 (2016) [arXiv:1602.05014 [hep-ph]].
- [9] A. Stoffers and I. Zahed, Phys. Rev. D **87**, 075023 (2013) [arXiv:1205.3223 [hep-ph]].
- [10] E. Shuryak and I. Zahed, Phys. Rev. D **89**, no. 9, 094001 (2014) [arXiv:1311.0836 [hep-ph]].
- [11] T. Kalaydzhyan and E. Shuryak, Phys. Rev. D **90**, no. 2, 025031 (2014) [arXiv:1402.7363 [hep-ph]].
- [12] Y. Qian and I. Zahed, Phys. Rev. D **92**, no. 10, 105001 (2015) [arXiv:1508.03760 [hep-ph]].
- [13] D. E. Kharzeev and E. M. Levin, arXiv:1702.03489 [hep-ph].
- [14] O. Nachtmann, Annals Phys. **209**, 436 (1991); O. Nachtmann, In *Cambridge 1995, Confinement physics* 27-69
- [15] Y. Qian and I. Zahed, arXiv:1211.6421 [hep-ph].
- [16] U. Gursoy, E. Kiritsis, L. Mazzanti, G. Michalogiorgakis and F. Nitti, Lect. Notes Phys. **828**, 79 (2011) [arXiv:1006.5461 [hep-th]].
- [17] A. H. Mueller and B. Patel, Nucl. Phys. B **425**, 471 (1994) [hep-ph/9403256]; A. H. Mueller, Nucl. Phys. B **437**, 107 (1995) [hep-ph/9408245]; G. P. Salam, Nucl. Phys. B **461**, 512 (1996) [hep-ph/9509353].
- [18] M. Luscher, Nucl. Phys. B **180**, 317 (1981); for a review see J. Greensite, Prog. Part. Nucl. Phys. **51**, 1 (2003) [arXiv:hep-lat/0301023].
- [19] M. Karliner, I. R. Klebanov and L. Susskind, Int. J. Mod. Phys. A **3**, 1981 (1988).
- [20] Y. Liu and I. Zahed, Phys. Rev. D **91**, no. 5, 055001 (2015) Erratum: [Phys. Rev. D **92**, no. 11, 119902 (2015)] [arXiv:1407.0384 [hep-ph]].
- [21] J. D. Bjorken, S. J. Brodsky and A. Scharff Goldhaber, Phys. Lett. B **726**, 344 (2013) [arXiv:1308.1435 [hep-ph]].
- [22] V. S. Fadin and L. N. Lipatov, Phys. Lett. B **429**, 127 (1998) [hep-ph/9802290].
- [23] L. Susskind, In *Teitelboim, C. (ed.): The black hole* 118-131 [hep-th/9309145]; G. T. Horowitz and J. Polchinski, Phys. Rev. D **55** (1997) 6189 [hep-th/9612146];
- [24] T. Damour and G. Veneziano, Nucl. Phys. B **568**, 93 (2000) [hep-th/9907030].
- [25] I. Iatrakis, A. Ramamurti and E. Shuryak, Phys. Rev. D **92**, no. 1, 014011 (2015) [arXiv:1503.04759 [hep-ph]].
- [26] J. F. Arvis, Phys. Lett. **127B**, 106 (1983).
- [27] P. Petreczky, Eur. Phys. J. C **43**, 51 (2005) [hep-lat/0502008].